Charge separation of excitons and the radiative recombination process in $PbBr_2$ crystals

Masanobu Iwanaga
Graduate School of Human and Environmental Studies, Kyoto University, Kyoto 606-8501, Japan

Masayuki Watanabe and Tetsusuke Hayashi
Faculty of Integrated Human Studies, Kyoto University, Kyoto 606-8501, Japan

(Received 24 May 2000)

The photoluminescence (PL) properties at low temperatures have been investigated in $PbBr_2$ crystals. We find that the blue-green PL band at 2.55 eV (BG band) originates from the intrinsic relaxed state of excitons. The analysis of the decay curve of the BG band reveals that the excitons relax into charge-separated pairs of a self-trapped electron and a self-trapped hole. The relaxation of an exciton results from the repulsive correlation between the electron and hole through acoustic phonons.

I. INTRODUCTION

Lead halide crystals, $PbCl_2$, $PbBr_2$, and PbI_2 crystals, decompose under ultraviolet (UV) light irradiation at and above room temperature.[1] In strong electron-phonon coupling systems, the band-to-band electronic transition generally causes lattice relaxation of the photocarriers, and induces lattice distortion. The halogen desorption and Pb-ion aggregation[1,2] have been thought to succeed the local lattice deformation. On the other hand, intense photoluminescence (PL) was reported for $PbCl_2$ and $PbBr_2$ at low temperatures.[3] The halogen desorption is suppressed at low temperatures, because ionic conductivity is proportional to $\exp(-U/k_BT)$, where U is the activation energy of halogen ions. Consequently, the lattice distortion is frozen in the crystals as a stable or metastable state, and self-trapped carriers at the distortion are probably related to the luminescence. Studying the luminescence, it is expected to clarify the relaxed states of carriers induced under photoexcitation into the fundamental absorption region.

$PbBr_2$ and $PbCl_2$ belong to the orthorhombic crystalline group D_{2h}^{16} which has low symmetry in the lattice configuration.[4] Photoelectron experiment[5] indicated that the upper edge of the valence band in PbX_2 is composed of hybrid orbits of $6s$ orbits of Pb^{2+} ions and np orbits of X^- ions ($X=$Br for $n=4$ and $X=$Cl for $n=3$), and that the middle of the valence band is mainly composed of np orbits of X^- ions. From polarized reflection spectra of both crystals, it was proposed that the exciton transition corresponds to the electric dipole transition from $6s$ to $6p$ states in Pb^{2+} ions within a rough approximation.[6–8] These experimental results have suggested that both crystals have similar electronic band structures: The valence band is composed of hybrid orbits of np orbits of X^- ions and $6s$ orbits of Pb^{2+} ions, and the conduction band is mainly composed of $6p$ orbits of Pb^{2+} ions.

Electron spin resonance (ESR) experiments revealed that x-ray[9] or γ-ray[10] irradiation on $PbCl_2$ at 77 K induces the lead-ion molecules Pb_2^{3+} which are two nearest-neighbor lead ions bonded covalently; a conduction electron bonds the two lead ions and localizes on the molecule. The localized electron is called a self-trapped electron (STEL). A self-trapped hole (STH) in $PbCl_2$ was also reported from a similar ESR experiment;[11] the STH is a hole localized on two nearest-neighbor halogen ions. Strong interactions of electrons and holes with acoustic phonons enable them to relax into STEL's and STH's, respectively.[12] The ESR experiments have implied that the interactions of electrons and holes with acoustic phonons play important roles in the relaxation processes in $PbCl_2$.

The intense PL at low temperatures in $PbBr_2$ and $PbCl_2$ gives much information on the relaxed states of the photocarriers. $PbBr_2$ and $PbCl_2$ are thought not only to have similar electronic band structures, but also to have similar relaxed states from the luminescent properties. According to Liidja and Plekhanov,[3] in $PbBr_2$, the blue PL band at 2.73 eV (B band) is induced under excitation into the exciton band and the blue-green PL band at 2.62 eV (BG band) under band-to-band excitation,[13] and, in $PbCl_2$, the ultraviolet PL band at 3.79 eV (UV band) is induced under excitation into the exciton band and the blue-green PL band at 2.55 eV (BG band) under band-to-band excitation. Because of the broad bands with large Stokes shifts, the origin of B band in $PbBr_2$ and that of UV band in $PbCl_2$ were attributed to self-trapped excitons.[3,15–17] However, any definite experimental result to support the assignments has not been found. In addition, the self-trapped exciton assigned to the origin of UV band is unlikely to relate to the STEL and the STH in $PbCl_2$; UV band disappears thermally at 25 K,[15,16] but both STEL's and STH's survive up to about 200 K.[9,11] Taking account of the inconsistency, another configuration of the self-trapped exciton was proposed;[17] in the configuration, an electron is self-trapped at one Pb^{2+} ion and a hole is bound in the orbit composed of $3p$ orbits of three Cl^- ions surrounding the Pb^{2+} ion at next nearest-neighbor sites. However, the self-trapping center of Pb^+ has not been demonstrated under excitation into the exciton band.

On the other hand, BG bands in the two crystals have a phosphorescent property; they decay in proportion to $t^{-m}(m\approx 1)$ under band-to-band excitation with vacuum-ultraviolet light.[18] From the decay curve of BG bands, both origins were attributed to direct tunneling recombination of a STEL with a shallow trapped hole.[18] It is expected that

STEL's and STH's are induced also in $PbBr_2$ under band-to-band excitation, though STEL's and STH's have not been reported yet.

According to the assignments, given so far, to the origins of PL bands, the relaxed states of photocarriers at low temperatures in $PbBr_2$ and $PbCl_2$ are as follows: excitons relax into self-trapped excitons, while the pairs of a free electron and a hole individually fall into the self-trapped states which are not coincident with the self-trapped exciton. That is, the relaxed states of electrons and holes are different with the excitation energy. However, the excited states of electrons are mainly composed of $6p$ orbits of Pb^{2+} ions and the states of holes are composed of hybrid orbits of np orbits of X^- ions and $6s$ orbits of Pb^{2+} ions; therefore, the excited states are thought to be almost independent of excitation energy.

To clarify the intrinsic relaxed states of photocarriers, we mainly focus the present study on the relaxation of excitons at low temperatures in $PbBr_2$. For the detailed study including the exciton absorption band, two-photon excitation is especially useful, because it induces electronic transitions between the states with the same parity; the selection rule, on the contrary, forbids the transitions under one-photon excitation. Moreover, two-photon excitation generates photocarriers almost uniformly in the crystal because of the small absorption coefficient, and is hardly influenced by the surface layer. On the other hand, one-photon excitation into the exciton band induces photocarriers only in the surface layer, because of the large absorption coefficient ($\approx 9 \times 10^5$ cm^{-1}).[19] According to the high ionic conductivity and the lattice defects which belong to Schottky type,[2] the density of the defects is estimated at higher than 10^{17} cm^{-3} in the surface layer. The PL bands mainly discussed in this study are B band and BG band. Although they are close in energy and overlap with each other, we can discriminate the two bands fully by using time-resolved measurements, so that the relaxation processes which induce B band and BG band can be discussed separately.

We present the PL properties in Sec. III, and discuss the origins of luminescence bands to clarify the intrinsic relaxed state of excitons in Sec. IV A. Moreover, we analyze decay curves by using the radiative recombination model and find that excitons relax into charge-separated pairs in Sec. IV B. To elucidate the origin of the exciton relaxation, we also discuss in Sec. IV C the interaction of excitons with acoustic phonons in comparison with the theoretical study by Sumi.[12]

II. EXPERIMENT

After $PbBr_2$ powder of 99.999% purity was purified under vacuum distillation, single crystals were grown with the Bridgman technique. The single crystal was cleaved in ab plane perpendicular to c axis (a,b,c: crystalline axes), and the cleaved plane was used for optical measurements. The typical dimension of the crystal was $8 \times 8 \times 3$ mm^3.

Light sources were an optical parametric amplifier (OPA) for the measurements of PL spectra and time-resolved PL spectra, and an optical parametric oscillator for those of two-photon excitation spectra. They were pumped by the third harmonics (3.4948 eV) with 10 or 30 Hz from Nd^{3+}:YAG (yttrium aluminum garnet) laser, and the pulsed light with 5 ns width was generated. The detector for the measurements of PL spectra was a charge-coupled device camera equipped with an amplifier. In the measurements of time-resolved PL spectra, the detector was gated by tuning the time width of applied voltage on the amplifier. The time resolution of the detector was 5 ns. The intensity of incident light was monitored, if necessary, by a reference photodiode in conjunction with an oscilloscope. In the measurements of decay curves, PL was induced by the pulsed light from the OPA, and the PL through a grating monochromator was detected by a photomultiplier tube (PMT) in conjunction with an oscilloscope. The light source for reflection spectra and excitation spectra was a Xe lamp equipped with a grating monochromator. In the measurements of polarized reflection spectra, the incident light was polarized by using a polarizer before it reached onto the sample surface. The backscattered reflection light from the surface was directly detected by a PMT in conjunction with a picoammeter. In the measurements of excitation spectra, PL through a grating monochromator was detected by the PMT. Optical measurements were performed below 8 K, except that temperature condition is particularly mentioned. The condition ensures that all the PL bands discussed in this study are independent of temperature.

III. RESULTS

Figures 1(a) and 1(b) show polarized reflection spectra for $\mathbf{E}\|a$ and $\mathbf{E}\|b$ configurations, respectively. The reflection spectra are in good agreement with previous reports.[6–8] The peaks at about 3.97 eV in Figs. 1(a) and 1(b) correspond to the excitonic transition from $6s$ to $6p$ states in Pb^{2+} ions.[6–8] The doublet structure at the peak for $\mathbf{E}\|b$ is due to crystalline field splitting.[6–8] Three PL bands are induced under excitation into the fundamental absorption region.[13] Figure 1(c) shows the blue PL band at 2.74 eV (B band) with a solid line, and the excitation spectrum observed at 2.95 eV with a dashed line. The excitation spectrum indicates that B band is mainly induced under excitation into the exciton band. Figure 1(d) shows the blue-green PL band (BG band) with a solid line, and the excitation spectrum observed at 2.38 eV with a dashed line. The intensities of PL spectra of B band and BG band are normalized at the peaks. The excitation spectra of the two bands are drawn to reflect the relative intensity. Figure 1(e) shows the red PL band at 1.7 eV (R band) with a solid line, and the excitation spectrum observed at 1.7 eV with a dashed line. The intensity of R band is about ten times weaker than that of BG band below 12 K. The excitation spectra of BG band and R band show that the two bands are induced under excitation into the whole fundamental absorption region. Arrows in the excitation spectra in Figs. 1(c)–1(e) stand for the excitation energies at which the corresponding PL bands were induced. Because both B band and BG band are induced at excitation energies between 4.0 and 4.2 eV, PL spectra induced in this energy range are composed of the two bands.

Figure 2(a) shows PL spectrum (solid line) induced under two-photon excitation at 3.947 eV (arrow), and the two-photon excitation spectrum (dots) for $\mathbf{E}\|a$ configuration. The two-photon excitation energy is the double of the incident photon energy. We measured a sequence of PL spectra for $\mathbf{E}\|a$ under two-photon excitation by tuning the incident photon energy from 1.928 to 2.221 eV. The two-photon excita-

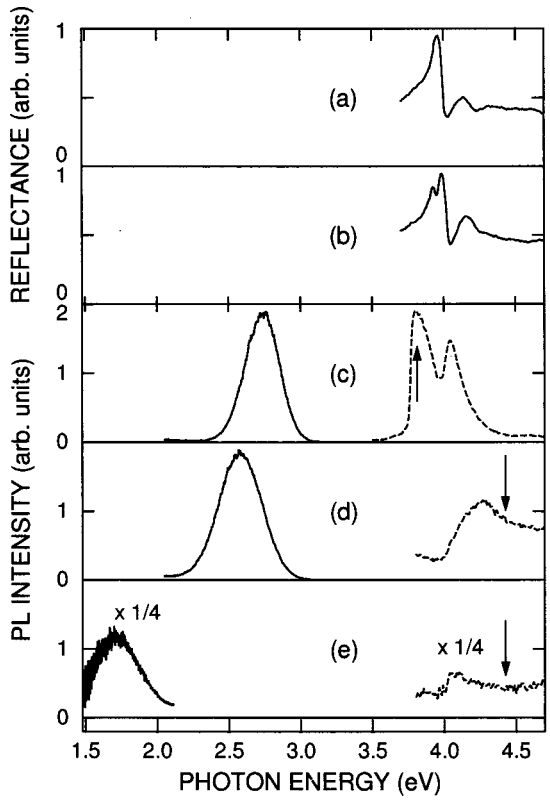

FIG. 1. Reflection, PL, and excitation spectra below 8 K. (a) and (b): Reflection spectra for $\mathbf{E}\|a$ and $\mathbf{E}\|b$ configurations, respectively. (c) PL spectrum of B band (solid line) under excitation into the exciton band at 3.814 eV (arrow), and the excitation spectrum observed at 2.95 eV (dashed line). (d) PL spectrum of BG band (solid line) under band-to-band excitation at 4.427 eV (arrow), and the excitation spectrum observed at 2.38 eV (dashed line). (e) PL spectrum of R band (solid line) under band-to-band excitation at 4.427 eV (arrow), and the excitation spectrum observed at 1.7 eV (dashed line).

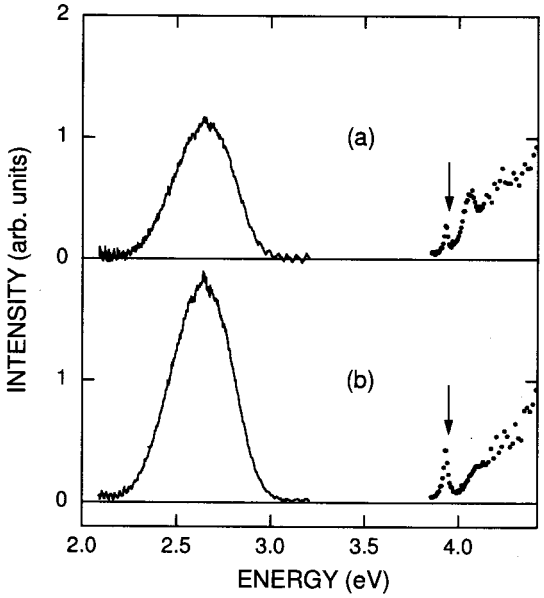

FIG. 2. PL spectra (solid lines) under two-photon excitation into the exciton band at 3.947 eV (arrows, the incident photon energy is 1.9737 eV), and the two-photon excitation spectrum (dots) at 2 K. (a) $\mathbf{E}\|a$; (b) $\mathbf{E}\|b$.

tion spectrum was obtained by dividing the integrated PL intensity by the mean square intensity of corresponding incident light. Figure 2(b) shows similar results for $\mathbf{E}\|b$ configuration. The PL spectrum was induced under two-photon excitation at 3.947 eV (arrow). The two-photon excitation spectrum for $\mathbf{E}\|b$ was obtained by the same procedure as for $\mathbf{E}\|a$. The PL spectra under two-photon excitation are resolved into BG band and B band as described in Fig. 4(b).

Two-photon excitation spectrum is regarded as two-photon absorption spectrum, as long as the quantum efficiency of PL is independent of excitation energy. The excitation spectra in Figs. 2(a) and 2(b) show different structures for $\mathbf{E}\|a$ and $\mathbf{E}\|b$. The difference is due to the electronic band structures dependent on the crystalline anisotropy. The discrete absorption at 3.932 eV in Figs. 2(a) and 2(b), and at 4.07 eV in Fig. 2(a) are ascribed to the transitions to the excitonic states. From the two-photon excitation spectra, the exciton absorption band in $PbBr_2$ is in the region where excitation energy is between 3.8 and 4.1 eV, and the band gap energy is about 4.1 eV.

Figure 3 shows decay curves of PL, represented with the log-log scale. Curve (a) is the decay curve under excitation into the exciton band at 3.960 eV, observed at 2.7 eV. From the energies of excitation and observation, curve (a) is regarded as the decay curve of B band. B band decays exponentially with the decay time of 3 μs. Curve (b), denoted by a solid line, is the decay curve of PL under band-to-band excitation at 4.349 eV, observed at 2.6 eV. Curve (b) is almost that of BG band from the energies of excitation and observation. A dashed line is the calculated curve of BG band derived in Sec. IV B. The decay curve of BG band is almost proportional to t^{-1} for $t>10$ μs. This result is consistent with the previous report[18] which showed that BG band decays nearly in proportion to t^{-1} for $t\geqslant 200$ μs. Curve (c), denoted by a solid line, is the decay curve of PL under two-photon excitation into the exciton band at 3.954 eV, observed at 2.6 eV. A dotted line shows the decay curve of B band, and a dashed line that of BG band. Curve (c) is composed of the two curves, and therefore suggests that the PL spectra consists of BG band and B band. However, only BG band is observed in the time range longer than 500 μs. The two PL bands can be, indeed, discriminated by the time-resolved measurements of PL spectra.

Figure 4 shows PL and time-resolved PL spectra. A solid line in Fig. 4(a) shows the PL spectrum under band-to-band excitation at 4.427 eV. A dashed line shows BG band obtained by the time-resolved measurement in which the gate for the detector was tuned on the time range 1 ms$\leqslant t \leqslant$100 ms. The spectrum of BG band was drawn to fit the low-energy tail of the PL spectrum. A dotted line denotes the difference between the PL spectrum and the spectrum of BG band. The difference spectrum is in good agreement with B band in Fig. 1(c). Figures 4(b) and 4(c) were obtained by the same procedure as in Fig. 4(a). The spectra in Fig. 4(b) are induced under two-photon excitation into the exciton band at 3.947 eV, and those in Fig. 4(c) under one-photon excitation into the exciton band at 3.935 eV. Dotted lines in Figs. 4(b) and 4(c) are also in good agreement with B band.

From the time-resolved PL spectra in Fig. 4, we can accurately define the PL band at 2.55 eV with 0.33 eV full

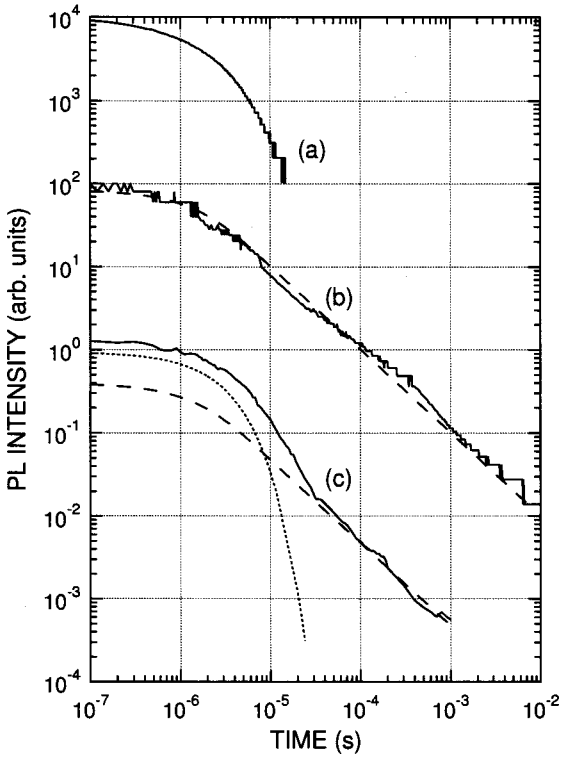

FIG. 3. Decay curves of PL below 8 K. (a) Decay curve of B band under excitation into the exciton band at 3.960 eV, observed at 2.7 eV. (b) Decay curve of BG band under band-to-band excitation at 4.349 eV, observed at 2.6 eV (solid line). Dashed line: the calculated curve of BG band. (c) Decay curve under two-photon excitation into the exciton band at 3.954 eV, observed at 2.5 eV (solid line). Dashed and dotted lines: the calculated curve of BG band and the decay curve of B band, respectively.

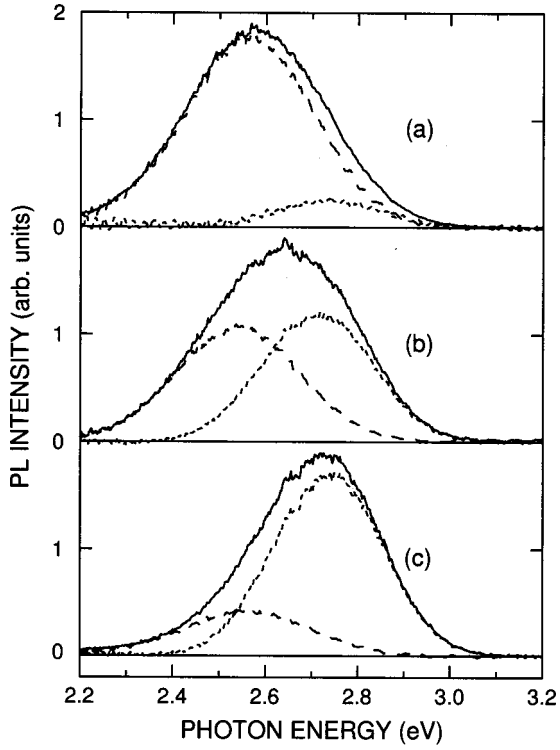

FIG. 4. PL and time-resolved PL spectra below 8 K. (a) PL spectrum under band-to-band excitation at 4.427 eV (solid line). (b) PL spectrum under two-photon excitation into the exciton band at 3.947 eV (solid line). (c) PL spectrum under one-photon excitation at 3.935 eV (solid line). Dashed lines are the time-resolved PL spectra. Each dotted line is the difference between each PL spectrum and the corresponding time-resolved PL spectrum.

width at half maximum as BG band. BG band is induced under excitation into the whole fundamental absorption region including the exciton absorption.

We measured the temporal evolution of PL spectra under one-photon excitation into the exciton band to examine whether the t^{-1}-dependent BG band is induced. Figure 5 shows the temporal evolution of PL spectra under the excitation at 3.935 eV. The delay time from the incident pulsed light was fixed at 18 μs, and the gate width was tuned from 10 μs to 99 ms. The delay time was chosen to make the influence of B band small. The peak of the spectra shifts toward lower energy as the gate width becomes longer. The peak reaches 2.57 eV in the end, and the PL spectrum is almost in agreement with BG band. In Fig. 6, the PL intensity at 2.5 eV in Fig. 5 (closed circle) is plotted against the logarithm of gate width w. A dashed line in Fig. 6 is a linear function of logarithm of w, and fits the data points in the range $w \geqslant 350$ μs. If PL decays in proportion to t^{-1}, the intensity $I(w)$ integrated over the interval $[t_0, w+t_0]$ is given by $I(w)=A\ln(w+t_0)+B$, where t_0 is the fixed delay time, and A and B are constants. The term $\ln(w+t_0)$ can be replaced by $\ln(w)$ under the condition $w \gg t_0$, so that $I(w)$ becomes a linear function of $\ln(w)$, namely, $I(w)=A\ln(w)+B$. Thus, the temporal evolution of PL spectra shows that the t^{-1}-dependent BG band is induced under one-photon excitation into the exciton band.

We examined the decay of PL in the short time range $t \leqslant 10$ μs. Figure 7 shows the time-resolved PL spectra under band-to-band excitation at 4.427 eV: The gate width was fixed at 1 μs and the delay time was taken at (a) 0 s, (b) 1 μs, and (c) 2 μs. The PL spectra were resolved, like Fig. 4, into BG band (dashed line) and B band (dotted line). It was found, from the analysis of a sequence of the resolved PL spectra, that BG band decays exponentially in the range $t \leqslant 6$ μs. The decay time is (1.2 ± 0.1) μs. The same examinations at different gate widths, 0.5, 0.8, and 1.2 μs, also gave the same decay time.

In Fig. 8, the logarithm of integrated PL intensity is plotted against the logarithm of excitation power of incident light. The PL was induced under two-photon excitation into the exciton band at 3.932 eV. The PL spectra were resolved into BG band and B band, like Fig. 4. The integrated intensity of BG band (closed circle) is proportional to the square of excitation power. A dashed line is a quadratic function of the excitation power, drawn for a guide to the eye. The response ensures that BG band is induced by two-photon absorption. On the other hand, the intensity of B band (cross) is not proportional to the square of excitation power, but shows a saturating tendency.

BG band exchanges into R band with raising temperature T. As T increases higher than 12 K, the intensity of BG band becomes weak. BG band finally disappears above 30 K, and R band is induced with high quantum efficiency for 30 K $\leqslant T \leqslant$ 50 K.

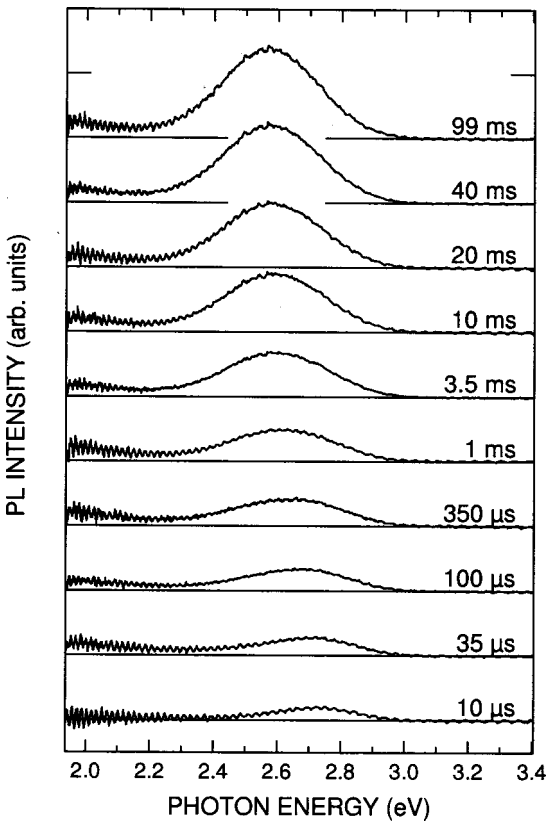

FIG. 5. Temporal evolution of PL spectra at 8 K induced under one-photon excitation into the exciton band at 3.935 eV. The gate width was tuned from 10 μs to 99 ms. The delay time was fixed at 18 μs.

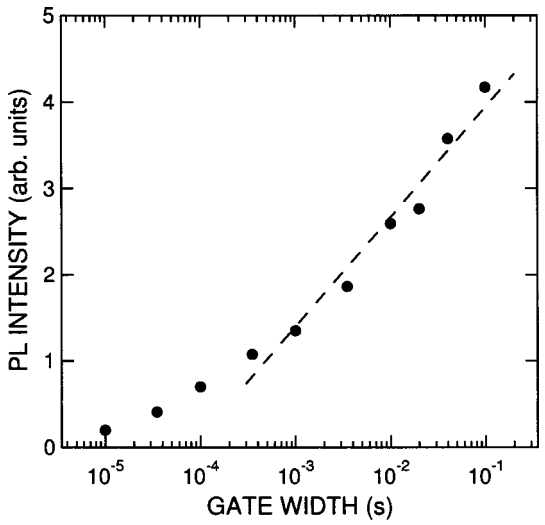

FIG. 6. Plot of PL intensity at 2.5 eV in FIG. 5 against the logarithm of gate width. Dashed line: a linear function of logarithm of gate width w.

IV. DISCUSSION

A. Origins of PL bands

We first discuss the PL properties to clarify intrinsic luminescence band in $PbBr_2$. Extrinsic luminescence bands due to lattice defects or impurities are usually induced under excitation into and mainly below the exciton band. Such extrinsic luminescence was reported in well-studied alkali halide crystals.[20]

Excitation spectrum of B band in Fig. 1(c) shows that B band is induced under excitation into and below the exciton band, and the quantum efficiency heavily decreases under band-to-band excitation. Moreover, as shown in Fig. 8, the intensity of B band under two-photon excitation is not proportional to the number of excitons induced by two-photon absorption, but saturates with increasing the excitation power. These results indicate that B band has signs of extrinsic luminescence. One of the plausible origins is the localized excitons perturbed by the lattice defects that exist densely in the surface layer. One-photon excitation into the exciton band induces excitons mostly in the surface layer, because of the large absorption coefficient.[19] Further results and discussion were reported elsewhere.[21] From now on, we do not deal with B band in the discussion.

BG band is induced under excitation into the whole fundamental absorption region including exciton absorption as shown in Figs. 1(d), 2, 4, and 5. The intensity of BG band under two-photon excitation into the exciton band is proportional to the square of incident light power as shown in Fig. 8. These results indicate that BG band is intrinsic in $PbBr_2$ and, in particular, the trapped electrons or holes which relate to BG band are self-trapped electrons or holes. BG band decays exponentially for $t \leqslant 6$ μs, while in proportion to t^{-1} for sufficiently large t as shown in Figs. 3, 6, and 7. The measured decay curves can be well explained by the recombination model, which contains a tunneling process of a STEL or a STH, as described in Sec. IV B. From the model, we ascribe the origin of BG band to the radiative recombination of the pairs either of which has tunneled toward the other.

R band is, as shown in Fig. 1(e), induced under excitation at higher energies than the energy of exciton absorption. The intensity of R band increases instead of the decrease in the intensity of BG band at temperatures higher than 12 K. These results indicate that R band also originates from intrinsic relaxed state of excitons, probably, self-trapped excitons. However, the PL spectra in Figs. 1(d) and 1(e) show that the intensity is much weaker than that of BG band below 12 K. Therefore, the relaxed state responsible for BG band corresponds to the dominant relaxed state of excitons at the low temperature.

B. Analysis of decay curves

We derive the decay curve of BG band from a radiative recombination model. The model describes the recombination process of a nearest-neighbor pair of a STEL and a STH separated by distance R: After either a STEL or a STH tunnels toward the other, the pair recombines with the decay time τ. In this context, the tunneled pair can be regarded as a kind of exciton accompanying with lattice distortion, namely, a self-trapped exciton, although the detailed structure has not been clarified yet. The formation of the self-trapped exciton is supported from the result that all the time-resolved PL spectra in which B band is completely removed have the same spectral shape as BG band, irrespective of the delay time.

Similar models containing a tunneling process were proposed to analyze the decay curves in doped alkali halide

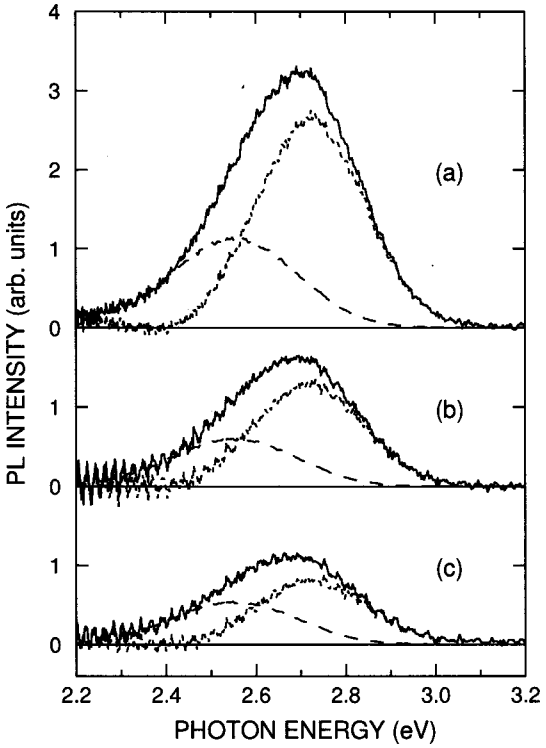

FIG. 7. Time-resolved PL spectra at 6 K under band-to-band excitation at 4.427 eV (solid line). The gate width was fixed at 1 μs and the delay time was taken at (a) 0 s, (b) 1 μs, and (c) 2 μs. Dashed and dotted lines: PL spectra of BG band and B band, respectively.

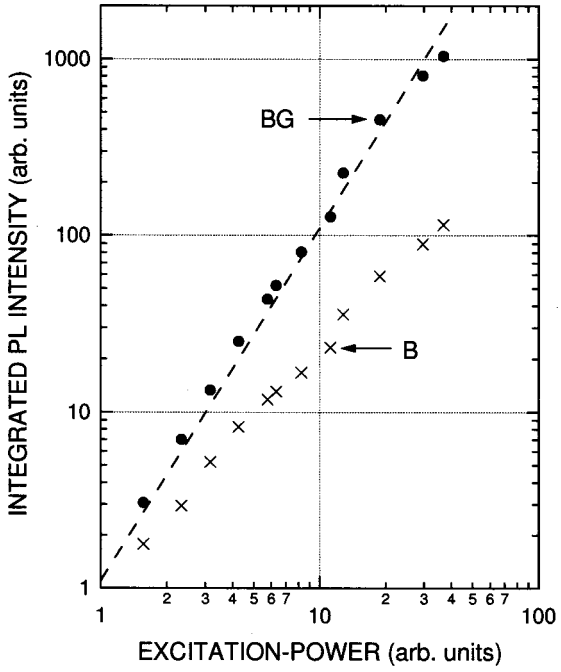

FIG. 8. Plot of the integrated PL intensity of BG band (closed circle) and B band (cross) against the excitation power. The PL bands were induced at 2 K under two-photon excitation into the exciton band at 3.932 eV. Dashed line: a quadratic function of excitation power, drawn for a guide to the eye.

crystals.[22,23] In these cases, the probability per second, $p(R)$, for the nearest-neighbor pairs separated by distance R to recombine is given by $p(R) \propto \exp(-\alpha R)$, where α is a constant. The density of nearest-neighbor pairs $n(\mathbf{R})$ was assumed to be random[22,23] or restricted only to one direction,[23] where $\mathbf{R}$ is the vector from the trapped electron to the STH (V_k center).

In the present study, we assume the following three hypotheses modified from the previous studies. The first hypothesis is that the rate $p(R)$ is the rapidly decreasing function of distance R, given by

$$p(R) = \frac{1}{\tau} \exp[-\alpha(R - R_0)], \tag{1}$$

where R_0 is the minimum distance of the nearest-neighbor pair of a STEL and a STH and $R \geqslant R_0$, α a constant, and τ the radiative decay time of the pairs separated by R_0. Equation (1) implies that the pairs separated by R_0 are responsible for the exponential decay in the short time range. Indeed, BG band decays exponentially with the decay time of 1.2 μs in the short time range $t \leqslant 6$ μs as shown in Fig. 7. We set $\tau = 1.2$ μs. The pair separated by R_0 can be regarded as the self-trapped exciton with the decay time τ. Equation (1) also shows that the rate $p(R)$ decreases rapidly if $R > R_0$. The dependence of $p(R)$ on R reflects the process that either a STEL or a STH moves, by tunneling, to the site separated by R_0 from the other. The radiative recombination following the tunneling is responsible for the t^{-1}-dependent part of decay curve.

The second hypothesis is that the total excited density is small enough. That is,

$$\frac{N_0 R_{max}^3}{V} \ll 1, \tag{2}$$

where N_0 is the total number of excited pairs, R_{max} the maximum distance of the pairs, and V the volume of area in which the pairs are induced under photoexcitation.

The third hypothesis is that the density of nearest-neighbor pairs $n(\mathbf{R})$ is the isotropic and decreasing function given by

$$n(\mathbf{R}) = \frac{N_0}{4\pi R_n R^2}, \tag{3}$$

where $R = |\mathbf{R}|$ and R_n is a normalization constant with a dimension of distance, satisfying $\int n(\mathbf{R}) d^3\mathbf{R} = N_0$. Equation (3) implies the physical picture that the electron and the hole which relax, respectively, into a STEL and a STH will not separate far away. That is, it is unlikely that each mean free path of the electron and the hole is far longer than R_0.

From the above three hypotheses, the decay curve $I(t)$ can easily be derived as follows. The number of the pairs in the radius interval $(R, R+dR)$ is equal to $n(R) 4\pi R^2 dR$ $[= (N_0/R_n) dR]$. The number of the pairs surviving at time t, $N(t)$, is then expressed by

$$N(t) = \int_{R_0}^{R_{max}} \frac{N_0}{R_n} \exp[-p(R)t] dR.$$

The PL intensity of BG band $I(t)$ is proportional to $-dN(t)/dt$, and given by

$$I(t)=\frac{A}{t}\{\exp[-p(R_{max})t]-\exp(-t/\tau)\},$$

where A is a proportionality constant. Under the condition that $\alpha=1/R_0$ and $R_{max}=15R_0$, one finds that $\exp[-p(R_{max})t]\approx 1$ for $t\leqslant 100$ ms, so that the intensity is simply written as

$$I(t)=\frac{A}{t}[1-\exp(-t/\tau)]. \tag{4}$$

In particular, $I(t)\propto t^{-1}$ for $10\tau\leqslant t\leqslant 100$ ms. It is to be noted that the R_{max} under the condition is the order of several nanometers, because R_0 is regarded as the radius of the self-trapped exciton. Furthermore, the R_{max} and the estimated values N_0, V in the experiments satisfy hypothesis (2).

The dashed line which fits curve (b) in Fig. 3 is the calculated curve $I(t)$ given by Eq. (4). Curve (c) in Fig. 3 was fitted with a single parameter A on the long time range where curve (c) is proportional to t^{-1}. The difference of measured curve (c) and the calculated curve $I(t)$ (dashed line) is in agreement with the decay curves of B band (dotted line). Thus, curve (c) is found to be composed of the decay curves of BG band and B band. This analysis confirms that charge-separated pairs of a STEL and a STH are induced even under excitation into the exciton band.

C. Exciton-acoustic phonon interaction

Free excitons and self-trapped excitons have been found and extensively investigated in many crystals of semiconductors and insulators. However, exciton relaxation into the pair of a STEL and a STH, to our knowledge, has not been found experimentally. Our experimental results and the analysis of the decay curve indicate that the exciton in $PbBr_2$ separates into the pair of a STEL and a STH in the intrinsic relaxation process. The physical origin of the charge separation of an exciton can be described by exciton-acoustic phonon interaction.[12]

The interaction is explained in the picture that an electron and a hole interact with acoustic phonons individually, being bound with each other by Coulomb attractive force. The interaction terms of an electron and a hole with acoustic phonons are proportional to the deformation potentials. The theoretical analysis by Sumi[12] showed that an exciton in the acoustic phonon field takes, within the adiabatic approximation, four possible relaxed states classified by the coupling constants and the ratio of the effective masses of the carriers: Corresponding to the lowest energy state of the exciton-acoustic phonon coupled system, an exciton becomes either of the free exciton, the large-radius self-trapped exciton, the small-radius self-trapped exciton or the pair of a STEL and a STH. In particular, separation of an exciton into the pair of a STEL and a STH originates from two factors, namely, the absolute values and the signs of deformation potentials: The large absolute values are responsible for the strong interaction to induce the self-trapping of the electron and the hole, and the opposite signs are for the repulsive correlation between them in the acoustic phonon field.

From the theoretical result, the exciton relaxation in $PbBr_2$ is ascribed to the repulsive correlation between the electron and hole through acoustic phonons. The same relaxation is also expected in $PbCl_2$, though a similar study on $PbCl_2$ has not been reported yet. The physical origin of the signs of the deformation potentials is probably the key to elucidate the mechanism to cause charge separation of an exciton, although no definite assignment to the factors which determine the signs has been reported so far. The low crystalline symmetry of $PbBr_2$ may be one of the factors.

V. CONCLUSION

The charge separation of excitons, namely, the relaxation of excitons into unbound, spatially isolated pairs of a STEL and a STH is found experimentally by studying the PL properties at low temperatures in $PbBr_2$. We ascribe the relaxation of excitons to the repulsive correlation between the electron and hole through acoustic phonons which couple strongly with the carriers, from the comparison with the theoretical result by Sumi.[12] The analysis using the radiative recombination model, which fits the measured decay curves well, reveals that the charge-separated pairs of a STEL or a STH recombine after either of them tunnels toward the other.

From the similar analysis, the pairs of a free electron and a hole are also found to relax into charge-separated pairs. Therefore, we conclude that the intrinsic relaxed state of carriers in $PbBr_2$ is independent of excitation energy.

ACKNOWLEDGMENT

We wish to thank Dr. M. Kitaura for valuable comments and the information on crystal growth.

[1] J.F. Verwey, J. Phys. Chem. Solids **31**, 163 (1970).
[2] J.F. Verwey and J. Schoonman, Physica (Amsterdam) **35**, 386 (1967).
[3] G. Liidja and VL. Plekhanov, J. Lumin. **6**, 71 (1973).
[4] R. W. G. Wyckoff, *Crystal Structures*, 2nd ed. (Wiley, New York, 1963), Vol. 1.
[5] J. Kanbe, H. Onuki, and R. Onaka, J. Phys. Soc. Jpn. **43**, 1280 (1977).
[6] A.F. Malysheva and V.G. Plekhanov, Opt. Spectrosc. **34**, 302 (1973) [Opt. Spektrosk. **34**, 527 (1973)].
[7] A.J.H. Eijkelenkamp and K. Vos, Phys. Status Solidi B **76**, 769 (1976).
[8] M. Fujita, H. Nakagawa, K. Fukui, H. Matsumoto, T. Miyagawa, and M. Watanabe, J. Phys. Soc. Jpn. **60**, 4393 (1991).
[9] S.V. Nistor, E. Goovaerts, and D. Schoemaker, Phys. Rev. B **48**, 9575 (1993).
[10] T. Hirota, T. Fujita, and Y. Kazumata, Jpn. J. Appl. Phys., Part 1 **32**, 4674 (1993).
[11] S.V. Nistor, E. Goovaerts, M. Stefan, and D. Schoemaker, Nucl. Instrum. Methods Phys. Res. B **141**, 538 (1998).
[12] A. Sumi, J. Phys. Soc. Jpn. **43**, 1286 (1977).
[13] Other luminescence bands were reported in Refs. 3, 14, and 17. The bands are extrinsic, because they largely depend on samples and are mainly induced under excitation in the lower energy

region than the exciton absorption.
[14] A.J.H. Eijkelenkamp, J. Lumin. **15**, 217 (1977), and earlier references cited therein.
[15] T. Fujita, K. Soeda, K. Takiyama, M. Nishi, and T. Hirota, J. Lumin. **28**, 267 (1983).
[16] K. Polák, D.J.S. Birch, and M. Nikl, Phys. Status Solidi B **145**, 741 (1988).
[17] M. Kitaura and H. Nakagawa, J. Lumin. **72-74**, 883 (1997).
[18] M. Kitaura and H. Nakagawa, J. Electron Spectrosc. Relat. Phenom. **79**, 171 (1996).
[19] V. Plekhanov, Phys. Status Solidi B **57**, K55 (1973).
[20] K. Kan'no, K. Tanaka, and T. Hayashi, Rev. Solid State Sci. **4**, 383 (1990).
[21] M. Iwanaga, M. Watanabe, and T. Hayashi, J. Lumin. **87-89**, 287 (2000).
[22] C.J. Delbecq, Y. Toyozawa, and P.H. Yuster, Phys. Rev. B **9**, 4497 (1974).
[23] T. Tashiro, S. Takeuchi, M. Saidoh, and N. Itoh, Phys. Status Solidi B **92**, 611 (1979).